Title

Alkaline activation of endogenous latent TGFβ1 by an injectable hydrogel directs cell homing for in situ complex tissue regeneration

Authors

Wang, Sainan
Niu, Yuting
Jia, Peipei
et al.

Publication Date

2022-09-01

DOI

10.1016/j.bioactmat.2021.12.015

Peer reviewed

Bioactive Materials 15 (2022) 316–329

Contents lists available at ScienceDirect

Bioactive Materials

journal homepage: www.keaipublishing.com/en/journals/bioactive-materials

Alkaline activation of endogenous latent TGFβ1 by an injectable hydrogel directs cell homing for in situ complex tissue regeneration

Sainan Wang [a,c,*,1], Yuting Niu [b,c,1], Peipei Jia [a], Zheting Liao [c], Weimin Guo [c], Rodrigo Cotrim Chaves [d], Khanh-Hoa Tran-Ba [e], Ling He [c], Hanying Bai [c], Sam Sia [d], Laura J. Kaufman [e], Xiaoyan Wang [a], Yongsheng Zhou [b], Yanmei Dong [a], Jeremy J. Mao [c,**]

[a] Department of Cariology and Endodontology, Peking University School and Hospital of Stomatology, Beijing, 100081, China
[b] Department of Prosthodontics, Peking University School and Hospital of Stomatology, Beijing, 100081, China
[c] Center for Craniofacial Regeneration, Columbia University, New York, NY, 10032, USA
[d] Department of Biomedical Engineering, Columbia University, New York, NY, 10027, USA
[e] Department of Chemistry, Columbia University, New York, NY, 10027, USA

ARTICLE INFO

Keywords:
Endogenous TGFβ1
Injectable alkaline hydrogel
Cell homing
Pulp-dentin complex
In situ tissue regeneration

ABSTRACT

Utilization of the body's regenerative potential for tissue repair is known as in situ tissue regeneration. However, the use of exogenous growth factors requires delicate control of the dose and delivery strategies and may be accompanied by safety, efficacy and cost concerns. In this study, we developed, for the first time, a biomaterial-based strategy to activate endogenous transforming growth factor beta 1 (TGFβ1) under alkaline conditions for effective in situ tissue regeneration. We demonstrated that alkaline-activated TGFβ1 from blood serum, bone marrow fluids and soaking solutions of meniscus and tooth dentin was capable of increasing cell recruitment and early differentiation, implying its broad practicability. Furthermore, we engineered an injectable hydrogel (MS-Gel) consisting of gelatin microspheres for loading strong alkaline substances and a modified gelatin matrix for hydrogel click crosslinking. In vitro models showed that alkaline MS-Gel controllably and sustainably activated endogenous TGFβ1 from tooth dentin for robust bone marrow stem cell migration. More importantly, infusion of in vivo porcine prepared root canals with alkaline MS-Gel promoted significant pulp-dentin regeneration with neurovascular stroma and mineralized tissue by endogenous proliferative cells. Therefore, this work offers a new bench-to-beside translation strategy using biomaterial-activated endogenous biomolecules to achieve in situ tissue regeneration without the need for cell or protein delivery.

1. Introduction

Regenerative medicine aims to repair or replace tissue defects resulting from trauma, tumor resection, infections or congenital anomalies. The development of stem cell biology and bioengineering has greatly advanced the field of regenerative medicine. However, the strategy to deliver ex vivo-manipulated stem cells or exogenous biochemical cues, such as recombinant growth factors, to wound sites has encountered many limitations, such as strict technical and regulatory requirements for cell manipulation, high cost and safety issues. These issues have prevented widespread clinical application. Therefore, stimulation of the body's natural regenerative capabilities via manipulation of endogenous stem cells and/or their niches is of growing interest for translational medicine [1–3].

Manipulation of endogenous growth factors to control endogenous stem/progenitor cells in situ may circumvent the problems caused by the delivery of exogenous cells or biochemical cues. Transforming growth factor beta 1 (TGFβ1) ubiquitously exists in the extracellular matrix in mammals and is widely involved in organ development, wound healing, tumor suppression and immunoregulation [4–7]. More importantly, TGFβ1 is capable of stem/progenitor cell recruitment [8]. However, TGFβ1 is secreted in a latent form consisting of a cytokine dimer and a

Peer review under responsibility of KeAi Communications Co., Ltd.
* Corresponding author. Department of Cariology and Endodontology Peking University School and Hospital of Stomatology, Beijing, 100081, China.
** Corresponding author.
E-mail addresses: bdkqwsn@bjmu.edu.cn (S. Wang), jmao@columbia.edu (J.J. Mao).
[1] These authors contributed equally to this work.

https://doi.org/10.1016/j.bioactmat.2021.12.015
Received 4 August 2021; Received in revised form 14 December 2021; Accepted 14 December 2021
Available online 23 December 2021

latency-associated propeptide (LAP), and its biological functions can only be performed after ligand activation [9]. Endogenous TGFβ1 may be harnessed as a potent growth factor to recruit stem cells to achieve in situ tissue regeneration, and its activation is the key step in the initiation of its physiological functions.

Methods to separate LAP for TGFβ1 activation include heating, ultrasonication, extreme pH exposure, ionizing radiation exposure, integrin binding and protease treatment [10–13]. Unfortunately, these methods have varied feasibility for in vivo application because of safety and practical concerns. Low-power laser (LPL) treatment-generated reactive oxygen species can activate endogenous TGFβ1 in vital pulp tissues for dentin repair [11]. However, only limited osteodentin repair has been observed rather than regeneration of the pulp-dentin complex [11]. Moreover, one-time laser treatment cannot guarantee long-term effects, and the limited penetration power of LPL prevents it from being applied for deep or large wound sites [14–16]. Acid/alkaline treatment can effectively activate latent TGFβ1 protein [17,18]. Platelets preincubated in acidic or alkaline buffers can release not only TGFβ but also other growth factors, such as platelet derived growth factor (PDGF) or vascular endothelial growth factor (VEGF) [19,20]. The pH changes caused by dental materials increase TGFβ1 release from platelet-rich fibrin in vitro [21]. Although acid/alkaline treatment is an appealing strategy, its application to modulate endogenous latent TGFβ1 for in situ tissue regeneration has not been systematically studied, and little is known regarding its performance for complex tissue regeneration in vivo.

Rationally designed biomaterials can be delivered to instructive microenvironments to promote tissue repair. Injectable hydrogels with good retention capacity in tissue defects have a wide range of tissue applications, and importantly, they are excellent candidates for loading and achieving controllable and sustained release of acidic/alkaline substances for effective endogenous latent TGFβ1 activation. However, commonly used hydrogels with good biocompatibility tend to form gels under neutral conditions (e.g., collagen gels) [22]. The crosslinkers grafted to hydrogel molecular backbones to promote hydrogel crosslinking (e.g., the click chemistry pairs of pendant tetrazine (Tr) and norbornene (Nb) [23] and amine and succinimidyl groups [24]) may lose their reactivity in strong acidic/alkaline environments and thus fail to function. Therefore, the engineering of a smart injectable hydrogel is needed, expecting to possess good crosslinking properties and to load strong acids/bases for controllable and sustained release to achieve endogenous TGFβ1 activation and in situ tissue regeneration. However, relevant research has not been reported.

In this study, we developed, for the first time, a biomaterial-based strategy for the alkaline activation of endogenous TGFβ1 for effective in situ tissue regeneration. First, we confirmed that the optimal alkaline activation condition of TGFβ1 in various tissue sources was pH 10 and that activated TGFβ1 from tissues could promote the homing and early differentiation of human bone marrow stem cells (hBMSCs). On this basis, we engineered an injectable alkaline hydrogel (MS-Gel, Scheme 1) consisting of gelatin microspheres (MSs) to load strong alkaline substances for endogenous TGFβ1 activation and a modified gelatin matrix

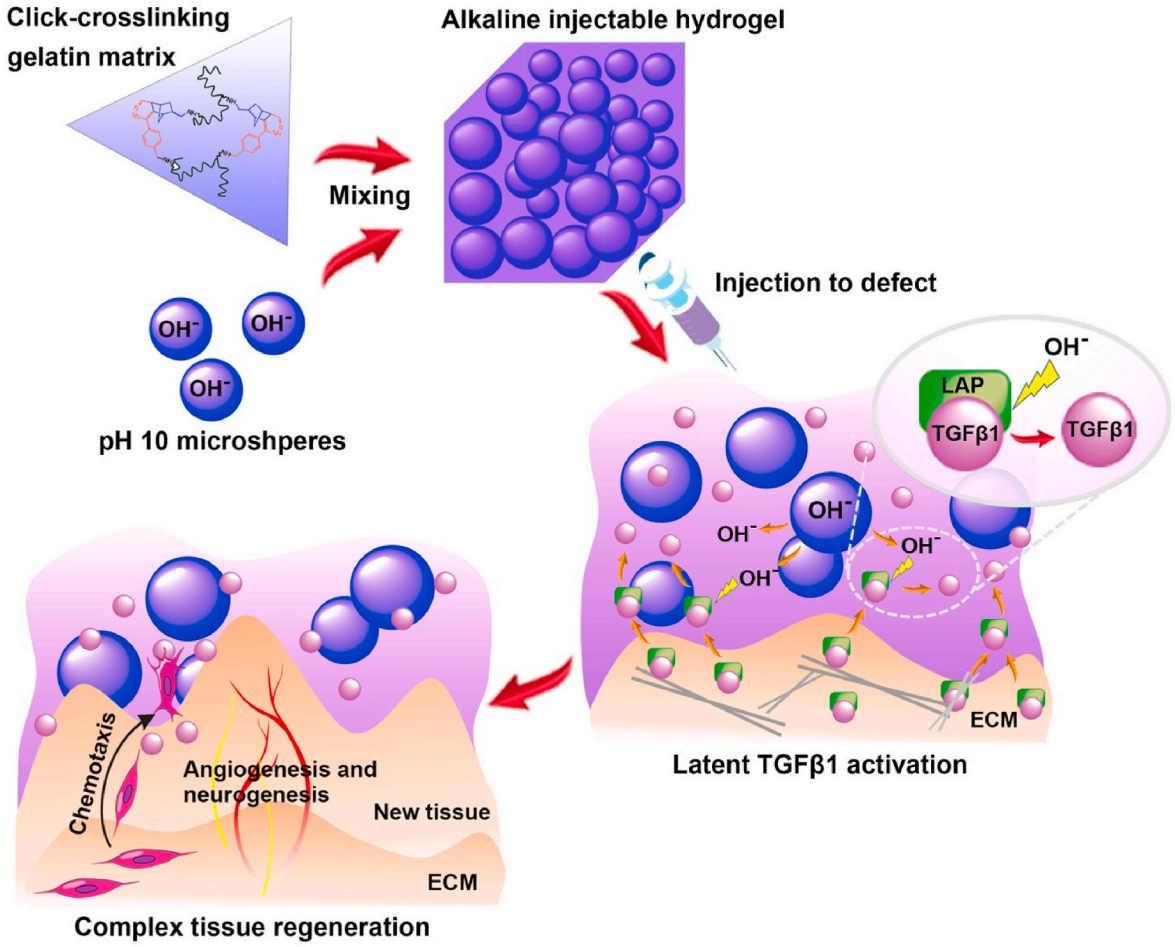

Scheme 1. Schematics of tissue repair by pH **10 MS-Gel activated endogenous TGFβ1**. An injectable alkaline hydrogel was composed by gelatin microspheres for loading strong alkaline substances and a modified gelatin matrix for hydrogel click crosslinking. After injection into the tissue defect, the alkaline substances reserved in the buffer pool of microspheres were able to diffuse into the entire hydrogel and activated endogenous latent TGFβ1 released from the extracellular matrix (ECM), thereby promoting mesenchymal stem cell (MSCs) recruitment/chemotaxis and tissue regeneration.

for hydrogel click crosslinking. In this system, alkaline substances reserved in the buffer pool of MSs were able to be sustainably diffused into the entire hydrogel and slowly released to surrounding tissues, maintaining a strong alkaline environment in a mild and controllable manner. Moreover, we demonstrated that this alkaline MS-Gel-activated dentin-derived TGFβ1 induced BMSC migration in vitro and facilitated the regeneration of complex tissues (neurovascular stroma and mineralized dentin) in both orthotopic and ectopic models. The strategy of biomaterial-based endogenous TGFβ1 activation achieved the goal of promoting complex tissue regeneration without the need for cell transplantation or exogenous growth factor delivery.

2. Materials and methods

2.1. Preparation and characterization of MS-Gel

2.1.1. Fabrication of a microfluidic flow-focusing device

The microfluidic circuit was firstly designed using Solidworks CAD software (Dassault Systems). A computer numerical control (CNC) milling program was created using Mastercam (CNC Software), per microfluidic circuit design and dimensions. The channel widths were 200 μm, and a 60 × 20 mm outline of the device was extracted from a 3.2 mm thick PMMA sheet using a Laser engraver (Universal Laser Systems, VLS 6.30). This cut out was then taken to a CNC machine (HAAS Super Minimill), where the microfluidic circuit was micromachined based on the CNC program. Milling conditions were optimized for the material type and tool dimensions. Fluidic ports were created using a drill press (Ellis), whereas drill bits were selected to match tubing outside diameter. Prior to assembly, the PMMA device was thoroughly cleaned by sonication and dried with nitrogen gas. Finally, the device was sealed using clear adhesive tape.

2.1.2. Fabrication of gelatin microspheres (MSs)

Gelatin MSs were fabricated though microfluidic method using microfluidic flow-focusing circuit. Respectively, the oil phase (20 wt% Span80 in mineral oil) and the aqueous phase (5 wt% gelatin solution) were injected into the inlets a (Fig. S6Aa) and b (Fig. S6Ab) of the microfluidic chip from 10 ml syringes (BD Biosciences) connected by plastic tubing (0.8 mm inner diameter and 1.6 mm outer diameter, C-Flex® laboratory tubing, Sigma). To avoid pre-injection gelation of the gelatin solution, the temperature was kept above 30 °C. The flow rate was set at 9 μL/min for the oil phase and 2.5 μL/min for the aqueous phase, under the control by syringe pumps (New Era). The mixture including gelatin microemulsions and mineral oil was collected in a container from the outlet (Fig. S6Ac) connected by another plastic tubing. In order to stabilize the microemulsions, the mixture was cooled down to 15 °C, where the microemulsions were kept as gel particles. The gelatin MSs were washed with ethanol and water after the crosslinking of gelatin microemulsions in 5% glutaraldehyde (Sigma) for 5 h, followed by blocking excessive aldehyde groups in 25 mM Glycine (Sigma) for 1 h. Following further washing, MSs were freeze-dried, and then kept in room temperature.

2.1.3. Amine group quantification

The amount of amine-group represents the active sites for modification, and its changes can be quantified by ninhydrin assay. Briefly, 100 μL of 20 mg/ml type B gelatin solution was mixed with 100 μL of (2 w/v%) ninhydrin solution in dimethyl sulfoxide (DMSO, Aladdin) for chromogenic reaction at 90 °C for 20 min. After the mixtures were cooled down to room temperature, 800 μL of DMSO was added to stop the reaction, and the absorbance at 570 nm was recorded using a microplate reader (ELX808, BioTek, VT). Glycine solutions from 2.5 to 25 mM were used to draw a standard curve.

2.1.4. Synthesis of Tetrazine/Norbornene-modified gelatin

The modification was conducted in 0.1 M 2-(N-morpholino) ethanesulfonic acid (MES) buffer, pH6 at 37 °C. For gelatin-tetrazine (GelTr) synthesis, 0.2 mmol of 5-[4-(1,2,4,5-Tetrazin-3-yl) benzylamino]-5-oxopentanoic acid (Tr) was first dissolved, followed by adding 0.04 mmol of N-hydroxysuccinimide (NHS; Sigma-Aldrich) to stabilize the reaction for 10 min, and by mixing 0.08 mmol of N-(3-Dimethyl aminopropyl)-N′-ethylcarbodiimide hydrochloride (EDC; Sigma) to activate the carboxylic groups in Tr for 20 min. Type B gelatin (1.2 g, Sigma) was added dropwise at a final concentration of 1% w/v. The reaction was stirred at 37 °C for 16 h and then dialyzed in 12–14 kDa MWCO dialysis tubing (Sigma) for 3 days against deionized water. The purified GelTr polymers were sterile-filtered (0.22 μm) and freeze-dried. For gelatin-norbornene (GelNb) synthesis, a similar protocol was used but with substituting 5-norbornene-2-methylamine (Nb, Fisher Scientific) for the Tr at 2 mmol of Nb per gram of dry gelatin, and adding in EDC and NHS to reach a final molar ratio of 1:2:1 (Nb:EDC:NHS). GelTr and GelNb were then kept at −20 °C. For qualitatively determine the modifications, lyophilized products (unmodified gelatin, GelNb, and GelTr polymers) were dissolved in deuterium oxide (Sigma) at 15% w/v, and 1H NMR was performed on a 600 MHz NMR spectrometer (Varian) set at 40 °C to qualify the substitution of carboxylic acid side chains on gelatin by tetrazine and norbornene. The peaks at δ7.5, δ10.4 (s, 1H) and δ6.2–5.9 (m, 2H) were attributed to aromatic gelatin backbone, the aromatic proton on tetrazine and the alkene proton on norbornene, respectively.

2.1.5. Determination of tetrazine and norbornene attachment

FTIR spectra of Tr, GelTr and GelNb were collected using Thermo Scientific™ Nicolet™ 6700 FT-IR spectrometers. Each spectrum was obtained using the liquid form or solutions against a background measured under the same condition. Absorbance curves of Tr in different solutions were investigated for quantitative determination. Tr was dissolved in 0.1 M pH 6 MES buffer at 0.5 mg/mL, and it was scanned from 400 to 600 nm to identify its characteristic peak position. MES buffer was scanned as a control. GelTr and unmodified gelatin were dissolved in water at 1%w/v. The molar amount of Tr attached on gelatin backbone was determined from the Tr standard curve at the characteristic 518 nm peak. For Nb attachment, both GelNb (10% w/v) and Tr (0.5 mg/mL) were dissolved in MES buffer, followed by mixing 10-μL GelNb solution with different volumes of Tr solution and recording 400- to 600-nm absorbance curves. The Nb attachment was finally determined at the disappearance of the characteristic peak at 518 nm.

2.1.6. Degree of crosslinking (DCL)

The DCL of MSs and GelTr-GelNb gelatin matrix are calculated as follows: For MSs, the crosslinking is attributed to the reaction of glutaraldehyde with two adjacent amine-groups. Therefore, the maximal DCL for MSs is estimated to be half the number of amine-groups, and that is 250 nmol/mg ÷ 2 = 125 nmol/mg, based on the results from ninhydrin assay. For GelNb-GelTr gelatin matrix, the crosslinking is based on the reaction between Nb and Tr. Therefore, the maximal DCL is calculated as the below:

1. Tr attachment: 66 nmol/mg,
2. Nb attachment: 99 nmol/mg,
3. To reach the maximum crosslinking, the molar ratio between Tr and Nb should be 1:1. Therefore, 3 parts of GelTr will mix with 2 parts of GelNb, and DCL=(66x3+99x2)/(2 + 3)÷2 = 39.6 nmol/mg.

2.1.7. Synthesis of the pH 10 and pH 7.4 MS-Gel

To enable the an alkaline condition (pH 10) or a neutral condition (pH 7.4), bicarbonate/carbonate in 0.15 mol/L pH 10 Na_2CO_3–$NaHCO_3$ buffer or phosphate in 0.01 mol/L pH 7.4 PBS buffer with normal human osmotic pressure (Table S1) were loaded into the buffer pool of the MSs by diffusion in advance. Sodium bicarbonate solution at 1 mol/L was prepared, then its pH value was adjusted to 10 using 1 mol/L sodium hydroxide. The concentration of carbonate ions was fixed to 0.15 mol/L

using a volumetric flask to get 0.15 mol/L pH 10 Na_2CO_3–$NaHCO_3$ buffer. The solution was dripped onto MSs at a volume of 5 μL per mg of dry MSs. Upon complete swelling, loaded MSs were freeze-dried overnight and then composited with the mixture of 5% GelNb and GelTr solutions to yield a MS-Gel composite (MS-Gel, Fig. 1A), also at a volume of 5 μL of GelTr-GelNb gelatin matrix per mg of dry MSs. For the pH7.4 MS-Gel, the protocol was the same, except carbonate buffer at pH 10 was replaced with 0.1 M PBS at pH 7.4. Before complete gelation, the MS-Gel slurry was transferred into a 1 mL syringe and injected into prepared root canals. Surface topographies of MS-Gel was examined with Zeiss Supra 55VP scanning electron microscopy (SEM, Zeiss, Oberkochen, Germany).

2.1.8. Rheology of MS-Gel

An Anton Paar MCR 302 WESP rheometer was employed to probe hydrogel and MS-Gel using a rheometer with a built-in temperature and gap calibration. A Peltier element (Anton Paar, P-PTD200/GL) was used to maintain a constant temperature at 37 °C, set for at least 15 min before the experiments under equilibrated thermal conditions. All biomaterials, including 5% GelTr-GelNb gelatin matrix in pH 7.4 PBS or in 0.15 mol/L pH 10 bicarbonate buffer, and pH 7.4 or pH 10 MS-Gel with 4–6% gelatin matrix concentrations, respectively, were prepared by thorough mixing of all components prior to transferred onto rheometer. On average, this procedure took less than 120 s. Rheology measurements were performed with a 2-min delay following initiation of gelation. A metal parallel plate geometry (Anton Paar PP25, 25 mm in diameter) was utilized in oscillation mode. The gap size for each gel was determined as the gap at which a normal 1-N force was measured, with gap height ~0.1 mm for all samples. Storage, G', was monitored with strain amplitude $\gamma = 1\%$ and angular frequency $\omega = 10$ rad/s for 18 min. During these measurements, the normal force was maintained at ~1 N. Gap height was re-adjusted when normal forces exceeded 50% of the set value. Each data point was collected by averaging over 90 oscillations with a 15-sec interval. All measurements were repeated at least 3 times to demonstrate the reproducibility of sample preparation.

2.1.9. In vitro MS-Gel enzymatic degradation

For in vitro degradation tests, 50 μL of 5% MS-Gel was formed in 1.5 mL microcentrifuge tubes, and 1 mL of collagenase I (50 μg/mL) in 0.1 M PBS was added to the tubes for digestion in 37 °C with shaking. After

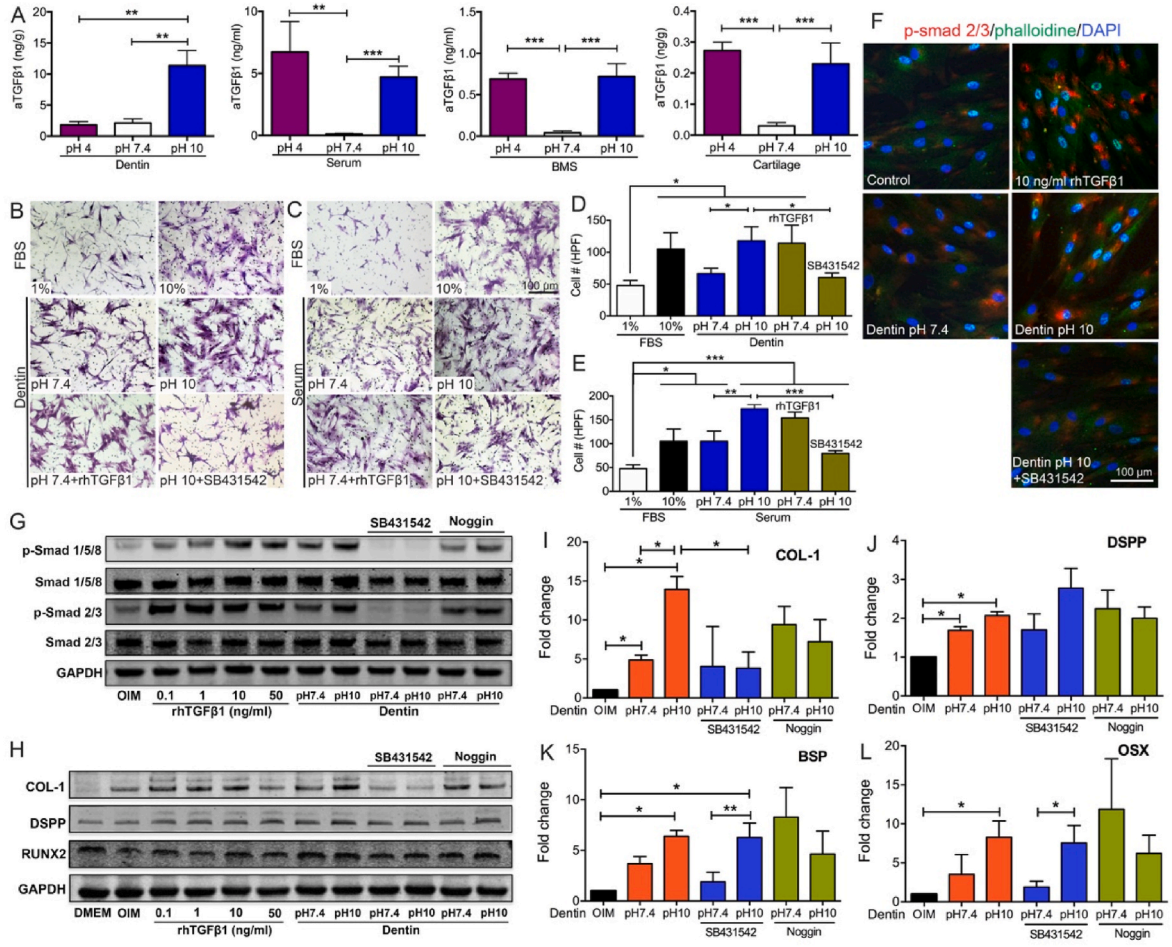

Fig. 1. Effects of acidity or alkalinity changes on latent TGFβ1 activation in various tissue sources for cell migration and differentiation. (**A**) ELISA was used to measure activated TGFβ1 in dentin extract, serum, BMS and cartilage extract treated at pH 4, pH 7.4 or pH 10. (**B and C**) Digital images of hBMSC migration exposed to 1% FBS, 10% FBS, 10% pH 7.4-treated human dentin extracts and serum, 10% pH 10-treated human dentin extracts and serum, 10% pH 7.4-treated human dentin extracts and serum with rhTGFβ1 equivalent to the concentration in pH 10-treated counterparts, 10% pH 10-treated human dentin extracts and serum with 10 μM SB431542. (**D and E**) Quantification of hBMSCs migration in (b) and (c). (**F**) Confocal microscopy images of phospho-smad 2/3 pathway activation after exposure to 10% FBS, 10 ng/ml rhTGFβ1, 10% pH 7.4-treated dentin extracts and 10% pH 10-treated dentin extracts with/without 10 μM SB431542. (red, phospho-smad2/3; green, phalloidin; blue, DAPI). (**G**) Western blot of the Smad pathway of hBMSCs exposed to osteogenesis induction medium (OIM); OIM supplemented with 0.1, 1, 10 and 50 ng/mL rhTGFβ1; and OIM supplemented with pH 7.4- and pH 10-treated dentin extracts with or without SB431542 and Noggin. (**H**) Western blot of COL-1, DSPP and RUNX2 protein expression in treated hBMSCs. (**I** to **L**) Real-time PCR of COL-1, DSPP, BSP and OSX gene expression in treated hBMSCs.

centrifugation, 500 μL of the liquid was collected at the indicated time points, and 500 μL of fresh enzyme solution was refilled. Pure enzyme solution, MSs only and 5% gelatin matrix only were used as controls. The protein concentrations were investigated using the BCA method and the absorbance was collected at 562 nm. Gelatin solutions with varied concentrations were used to depict a standard curve.

2.1.10. Young's modulus

The mechanical properties of the MS-Gel samples were measured by compression using a BioDynamics testing system (TA Instruments), following previously a reported procedure. Disc-shaped gel samples (3.5 mm × 2 mm) were prepared and immediately used for compression test. Tensile tests were done at 5% strain/min after preconditioning for 10 cycles (1–5% strain) at 0.5 Hz frequency. Four measurements were done for each gel group. The linear portion of each stress-strain curve was used to determine the compression modulus.

2.2. In vitro cell experiments

2.2.1. Cell culture

Human bone marrow mesenchymal stem cells (hBMSCs) (ATCC, PCS-500-012) were cultured in MSCs human Basal Medium (ATCC, PCS-500-030) with 1% penicillin/streptomycin (Sigma-Aldrich) and with or without 125 pg/mL FGF basic, 15 ng/mL IGF-1, 7% fetal Bovine Serum and 2.4 mM L-Alanyl-L-Glutamine (ATCC, PCS-500-041). A total of 5 independent hBMSCs samples were used (age range: 20–35 years old). Cells were incubated in a humidified incubator with 5% CO_2 at 37 °C. HBMSCs were passaged at 80% confluence, with medium change every 2 days. Less than passage 3 cells were used for all experiments.

2.2.2. Cell viability and proliferation on MS-Gel

HBMSCs (5×10^4 per well) seeded in 24-well plates were exposed to MSs at 1 mg/mL. Cell growth was observed under inverted microscope and recorded. For cell proliferation, hBMSCs (5×10^3 per well) seeded in 96-well plates were exposed to MSs for 1, 3 and 5 days, followed by cell number quantification with Cell Counting Kit-8 (CCK-8) (Sigma-Aldrich) at 450 nm absorbance. At least biological triplicates were performed per group for cell viability or cell proliferation. Fluorescent hBMSCs (5×10^4) were seeded on the surface of pH 10 MS-Gel after pH neutralization and cultured for 3 days. Cell growth on MS-Gel was viewed by confocal microscopy (Nikon A1RMP or Leica DMI6000B).

2.2.3. TGFβ1 release and activation

De-identified, surgically extracted healthy human teeth were obtained from Columbia University College of Dental Medicine clinic, following IRB approval. Periodontal and peri-apical soft tissues were removed by scalpel. Enamel and cementum were removed using high-speed diamond bur and dental pulp was extirpated. The remaining dentin was grinded into fragments and treated with 17% Ethylene Diamine Tetra-acetic Acid (EDTA) at pH 7.4 for 10 min, followed by washing with distilled water for three times. TGFβ1 was extracted from dentin fragments in acidic (Citric acid buffer, pH 4), neutral (PBS, pH 7.4) or basic (Na_2CO_3–$NaHCO_3$, pH 10) solutions at 1 g/mL. Supernatants were neutralized to pH 7.4 and sterilized through 0.22 μm filters before use. Dentin derived TGFβ1 release and activation in pH 4, pH 7.4 or pH 10 solution was measured by ELISA.

Fresh goat meniscus was cut into fragments. TGFβ1 was extracted from meniscus fragments in acidic (Citric acid buffer, pH 4), neutral (PBS, pH 7.4) or basic (Na_2CO_3–$NaHCO_3$, pH 10) solutions at 1 g/mL. Supernatants were neutralized to pH 7.4 and sterilized through 0.22 μm filters before use. Meniscus derived TGFβ1 release and activation in pH 4, pH 7.4 or pH 10 solution was measured by ELISA.

Human whole blood samples were collected from 5 donors aged from 25 to 35 years old. The whole blood was left undisturbed at room temperature for 30 min. Then the blood clots were removed by centrifuging at 1000 g for 10 min in a refrigerated centrifuge. The supernatant which is designated serum was collected, and apportioned into 0.5 ml aliquots with clean polypropylene tubes. Serum was stored at −20 °C before use. Fresh human bone marrow aspirate (Lonza) was centrifuged at 400 g × 10 min. The bone marrow supernatant (BMS) was collected and stored at −20 °C before use. To activate the latent TGFβ1, serum and BMS was adjusted to different pH values by adding 1 N HCl or 1 N NaOH for 30 min at room temperature. The concentrations of activated and total TGFβ1 in serum were measured by ELISA. All samples were neutralized (pH 7.2–7.6) and diluted to suitable levels before tests.

TGFβ1 concentration was measured using Human TGFβ1 Quantikine ELISA Kit (R&D Systems, Abingdon, Oxon, UK). Total TGFβ1 was tested by pre-treating with 20-μL, 1 N HCl per 100-μL sample and incubating at room temperature for 10 min to activate all latent TGFβ1 in samples, followed by pH neutralization with 20 μL 1.2 N NaOH/0.5 M HEPES per 100 μL sample. The concentrations of activated TGFβ1 by different pH values were measured without HCl pre-treatment. Assays were performed following manufacture's protocol in at least biological triplicates.

2.2.4. Dentin derived TGFβ1 release and activation by pH 7.4 or pH 10 MS-Gel

Periodontal and peri-apical soft tissues of obtained teeth were removed by scalpel. Human root dentin slices (~2 mm thickness) were prepared by transverse sectioning the cervical 1/3 of tooth root, with a diamond-edged blade at low speed while cooling with sterile PBS. The root canal was endodontically instrumented to remove dental pulp and predentin. Human tooth roots (7–8 mm in length) were prepared by removing the tooth crown at the cemento-enamal junction, followed by endodontic instrumentation to remove dental pulp and predentin, and enlargement of apical foramen to 1 mm by a series of K files. Then human dentin slices and roots were immersed in PBS with 200 U/mL penicillin-G, 200 μg/mL streptomycin for 2 h for sterilization, and treated with 17% EDTA at pH 7.4 for 10 min to remove the smear layer, followed by deionized water washing.

The durability of nonphysiological pH was conducted by infusing pH 10 MS-Gel or pH 10 alkaline solution into endodontically prepared root canals of human teeth, maintaining for up to 4 days. The pH changes were tested by pH test strips. The release of activated TGFβ1 from tooth slices was evaluated by filling with pH 7.4 and pH 10 MS-Gel, followed by incubation for 24 h and immersion in 2 mL PBS (Fig. 3B). Activated TGFβ1 released into PBS at 2 and 12 h was measured by ELISA in at least biological triplicates. Endodontically prepared tooth roots were also infused with the pH 7.4 or pH 10 MS-Gel followed by incubation for 24 h. The root canal's coronal end was sealed with Cavit (3 M ESPE), and the apex were immersed in 200 μL PBS (Fig. 3C), cumulatively released activated TGFβ1 from the apical foramen into PBS was measured by ELISA up to the tested 28 days.

2.2.5. Cell migration

Cell migration was tested with 8-μm pore size Transwell@ cell culture set (Corning). Following 12-hrs serum starvation, 1×10^5 hBMSCs suspension was plated in the insert in 750 μL basal medium with 1% fetal bovine serum (FBS, Gibico). In the lower chamber, 750 μL of basal medium was added, supplemented with 1% FBS, 10% FBS, 10% pH 7.4 treated samples with/without recombinant human TGFβ1 (rhTGFβ1, R&D Systems), 10% pH 10 treated samples with/without 10 μM SB431542 respectively. Following 16-hrs incubation, cells migrated to the lower filter were fixed with 4% paraformaldehyde for 30 min, stained with 0.1% crystal violet for 20 min and counted under a microscope using at least biological triplicates.

A 3D collagen gel was adopted for cell migration assay using 8-μm pore size Transwell@ cell culture insert (Corning). Prepared tooth slices infused with the pH 7.4 or pH 10 MS-Gel were encapsulated into 3 mg/mL type I collagen gel, with collagen gel alone as a negative control and 10 ng/mL rhTGFβ1-loaded collagen gel as a positive control. HBMSCs (1×10^5 per well) were seeded on the superior surface of the collagen gel.

Following 3-day culture, migrated cells were stained with DAPI and viewed by confocal microscopy. Migrated cell number at 50 μm from surface of the collagen gel was counted.

2.2.6. Live/dead cell assay

HBMSCs (5×10^4 per well) were first seeded in 24-well plates. To evaluate the safety of biomaterials, 50 μL of pH 10 or pH 7.4 MS-Gel was immersed into 200 μL of culture medium in transwell upper chambers, which was then inserted into the 24-well plates with cells. The pH value of the culture media was tested at 1 h and 24 h. In addition, hBMSCs were incubated in culture medium supplemented with 10 v/v% pH 7.4 dentin or pH 10 dentin extracts. Moreover, culture medium was adjusted to pH 9 or pH 10. The culture medium containing 30 μM H_2O_2 was used as a positive control. Following 24 h incubation, live/dead cell assay was performed (Molecular Probes, Leiden, The Netherlands). Briefly, calcein AM at 2-μM and Ethidium Homodimer III working solution at 4-μM was added, followed by 30-min incubation in dark at room temperature.

2.2.7. Immunofluorescence

To visualize the accumulation of phospho-Smad 2/3 in cells, 1×10^5 hBMSCs were seeded onto 12-mm glass coverslips in 24 well-plates. The culture medium was added, supplemented with 10% FBS, 10 ng/ml rhTGFβ1, 10% pH 7.4-treated dentin extracts, and 10% pH 10-treated dentin extracts with/without 10 μM SB431542, respectively. In 30 min, the attached cells were first fixed with 4% paraformaldehyde in PBS for 30 min, blocked in PBS with 5% rabbit serum and 0.3% Triton X-100 for 1 h at room temperature, and incubated with anti-phospho-Smad2/3 antibody in antibody buffer (1% bovine serum albumin and 0.3% Triton X-100 in PBS) overnight at 4 °C. Then, the cells were incubated with secondary anti-Rabbit IgG (H + L) F (ab')$_2$ Fragment (Cell Signaling Technology) in antibody buffer at room temperature for 1 h. After that, the cells were further incubated with FITC-phalloidin (Sigma Aldrich, MO) in antibody buffer at room temperature for another 1 h. Finally, the coverslips were mounted onto glass slides by Fluoroshield™ with DAPI (Sigma). The slides were viewed using a confocal laser scanning microscope (LSM710, Zeiss, Germany).

2.2.8. Western blotting

Following 12-hr serum starvation, hBMSCs were cultured in osteo-/odonto-genesis induction medium (OIM) with or without 0.1, 1, 10 and 50 ng/mL rhTGFβ1, pH7.4 or pH10 dentin extracts, 700 ng/mL Noggin (R&D Systems) or 10 μM SB431542 (Selleckchem). After 30-min or 7-day culture, cells were washed with ice-cold PBS followed by protein extraction in RIPA Lysis Buffer (Thermo Scientific) with Protease/Phosphatase Inhibitor Cocktails (Cell Signaling Technology). Proteins were separated on a NuPAGE® Novex® 4–12% Bis-Tris Protein Gel (1.0 mm), transferred to nitrocellulose membrane (Bio-Rad), and detected with *anti*-phospho-Smad 2/3 (ab52903, 1:500, Abcam), *anti*-Smad 2/3 (ab202445, 1:500, Abcam), *anti*-Smad 1/5/9 (ab66737, 1:500, Abcam), *anti*-phospho Smad 1/5/8 (ab3848, 1:500, Millipore), anti-COL-1 (ab34710, 1:500, Abcam), anti-DSPP (sc-73632, 1:200, Santa Cruz Biotechnology), *anti*-RUNX2 (ab76956, 1:500, Abcam), *anti*-GAPDH (sc-25778, 1:200, Santa Cruz Biotechnology) antibodies. Images were developed with IR fluorescence & Odyssey using corresponding secondary antibodies (LI-COR).

2.2.9. Quantitative RT-PCR

RNA was extracted by Trizol Reagent (Invitrogen) and reverse-transcribed using iScript cDNA synthesis kit (Bio-Rad). The cDNA was amplified with gene-specific primers (Applied Biosystems). Real-time quantitative RT-PCR was performed using TaqMan Assay Protocol (Applied Biosystems): hold for 2 min at 50 °C, hold for 10 min at 95 °C, and 50 cycles of melt for 15 s at 95 °C and anneal/extend for 1 min at 60 °C. All reactions were run in at least biological triplicates. COL-1, DSPP, BSP and OSX mRNAs were evaluated. The primer sets were listed in Table S2. Relative expression levels were calculated using the $2^{-\Delta\Delta CT}$ method and determined by normalizing to GAPDH.

2.3. In vivo animal experiments

2.3.1. Animal models

All animal experiments including rat and swine use, care and surgical procedures were approved by Columbia University Institutional Animal Care and Use Committee (IACUC). Prepared human tooth roots as described above were immersed in PBS with 200 U/mL penicillin-G, 200 μg/mL streptomycin for 2 h. Following drying with paper points, pH 7.4 or pH 10 MS-Gel was infused into root canals to allow gelation. Under general anesthesia with isoflurane, subcutaneous pockets were created by blunt lateral dissection skin incision in 8-wk-old nude rats. Tooth roots were implanted into the subcutaneous pockets. Each rat received two human tooth roots. Six weeks later, rats were euthanized to retrieve all implants.

A total of 5 Yucatan minipigs (weighting 30–33 kg, Sinclair Bio Resources, Windham, Maine) were sedated with Telazol and anesthetized by i.v. propofol at 2–5 mg/kg. Under deep anesthesia, minipigs were intubated with an endotracheal tube and a mechanical respirator, with anesthesia maintained by isoflurane and oxygen (1–5% with 2L O_2/min), and monitored by heart rate (EKG), pulse oxymetry and blood pressure. Minipigs received prophylactic cefazolin (22 mg/kg, IV). Bupivacaine (0.5%) was intramucosally injected for mental nerve block. A preoperative digital radiograph was taken. Dental pulp was mechanically exposed with sterile high speed round burs with sterile saline cooling, and extirpated, followed by aseptic root canal preparation with endodontic files to working length measured with apex locator and radiographs. EDTA irrigation was applied for 5 min, followed by saline washing and drying with sterile paper points. Then pH 10 or pH 7.4 MS-Gel was infused into endodontically prepared root canals by backfill, with pH 7.4 collagen gel as a control. After complete gelation, the access cavity was sealed with Cavit and composite resin (3 M ESPE).

2.3.2. Microcomputed tomography

The Yucatan minipig jaw bones with treated teeth were harvested in 3 months and scanned using micro-computed tomography (micro-CT, Skyscan 1272, Aartselaar, Belgium) at 100 kV source voltage, 100 μA source current, and at a spatial resolution of 7.4 μm. Reconstructions were performed using NRecon software (Skyscan, Aartselaar, Belgium). DataViewer (Skyscan, Aartselaar, Belgium) was used to re-slice the CT images along coronal and sagittal sections which were used to re-orient the CT slices to be perpendicular to the axis of the teeth. A region of interest was then generated to include the teeth and surrounding bones. The final images were axial slices of the region of interest, which was essentially a cut through dentin and root canals.

2.3.3. Histological staining

The teeth specimens were fixed in 4% paraformaldehyde for 24 h and then decalcified with decalcifiers (Rio Gold) for ~1 month, washed with distilled water, dehydrated and embedded in paraffin. Sections were coronally cut longitudinally and stained with hematoxylin and eosin, Masson's Trichrome and Immunofluorescence. For Immunofluorescence, randomly selected sections were blocked in 5% goat serum. Primary antibody including DSPP (sc-73632, 1:100, Santa Cruz Biotechnology), von Willebrand Factor antibody (vWF, ab6994, 1:100, Abcam), S100 (ab868, 1:100, Abcam) and PGP9.5 (ab8189, 1:50, Abcam) were incubated overnight at 4 °C. Following PBS washing, sections were incubated with secondary antibodies for 2 h at room temperature, washed and counterstained with DAPI (Sigma-Aldrich, St. Louis, MO). The same procedures were performed for negative controls but without primary antibodies.

2.4. Statistical analysis

All experiments were performed in at least biological triplicates. All

quantitative data were analyzed using one way ANOVA. $P \leq 0.05$ was considered statistically significant. *$P \leq 0.05$; **$P \leq 0.01$; ***$P \leq 0.001$.

3. Results

3.1. Acidic/alkaline activation of latent TGFβ1 in various tissue sources promoted cell migration and differentiation

The efficiency of acidic/alkaline activation of latent TGFβ1 in tissues was evaluated. Serum and bone marrow supernatant (BMS), two important extracellular fluids involved in tissue repair, and extracts from the meniscus (cartilage) and tooth dentin, two acellular extracellular matrices with low self-repair ability, were chosen for the TGFβ1 activation test. In all four groups, untreated samples at pH 7.4 possessed very low quantities of active TGFβ1 (dentin, 1.79 ± 0.33 ng/g; serum, 0.13 ± 0.03 ng/mL; BMS, 0.04 ± 0.01 ng/mL; and cartilage, 0.02 ± 0.01 ng/g). After alkaline activation at pH 10 for 0.5 h, TGFβ1 levels in all samples were significantly increased by up to 10–40 times (dentin, 11.34 ± 1.41 ng/g; serum, 4.70 ± 0.51 ng/mL; BMS, 0.72 ± 0.06 ng/mL; and cartilage, 0.23 ± 0.03 ng/g) (Fig. 1A). Interestingly, the treatment time and alkalinity (pH value) were very important for TGFβ1 activation. For example, for cartilage, when the treatment time was 0.5 h, the content of activated TGFβ1 increased continuously with increasing alkalinity. However, when the treatment time was extended to 16 h, the results indicated that active TGFβ1 may have degraded under strong alkaline conditions (pH ≥ 11) (Fig. S1). Although latent TGFβ1 was also activated under acidic conditions (pH 4) in some tissue sources (serum, 6.73 ± 1.42 ng/mL; BMS, 0.69 ± 0.03 ng/mL; cartilage, 0.27 ± 0.01 ng/g) (Fig. 1A), acid-dissolved calcium and phosphate ions (e.g., from dentin) may have recrystallized and precipitated on the tissue surface, preventing the release of TGFβ1 (2.11 ± 0.39 ng/g) (Figs. 1A and S2). Moreover, acidic conditions can enhance the activity of osteoclasts, affecting bone/cartilage repair [25]. Therefore, the alkaline activation of endogenous TGFβ1 at pH 10 was our focus in all subsequent experiments.

Cell chemotaxis and differentiation in response to alkaline-activated TGFβ1 from various tissues were then evaluated in vitro. Compared to the pH 7.4 counterparts, the addition of pH 10-treated serum or dentin extract induced more robust hBMSCs migration (Fig. 1B–E), and this migration could be prevented by SB431542 (a TGFβ inhibitor). Recombinant human TGFβ1 (rhTGFβ1) was then added to the pH 7.4-treated serum or dentin group to make their TGFβ1 content equivalent to that of their pH 10-treated counterparts and induced cell migration comparable to that in the pH 10 group. In addition, pH 10-treated BMS and cartilage extract also induced more hBMSCs and chondrocyte migration, respectively, than pH 7.4-treated samples (Fig. S3). Immunofluorescence images showed that pH 10-treated dentin extracts significantly increased the expression of p-Smad 2/3 in hBMSCs compared to their pH 7.4 counterparts (Fig. 1F). In addition, this increase could be hindered by SB431542. Western blot and RT-PCR results further confirmed that compared to their pH 7.4 counterparts, pH 10-treated dentin extracts in culture medium significantly activated the Smad 2/3 and Smad 1/5/8 pathways (Fig. 1G) and upregulated collagen I (COL-1) gene and protein expression (Fig. 1H and I). This upregulation was strongly prevented by SB431542 and slightly attenuated by Noggin (a bone morphogenetic protein antagonist). The quantified Western blot results are shown in Fig. S4. Furthermore, the gene and protein expression of dentin sialophosphoprotein (DSPP) and the osterix (OSX) and bone sialoprotein (BSP) genes in the pH 10 group were higher than in the control groups; however, SB431542 and Noggin did not hinder this upregulation (Fig. 1J-L). Live/dead assays showed that little cell death was caused by pH 10-treated dentin extract (Fig. S5). The above results imply that alkaline conditions at pH 10 can activate latent TGFβ1 in various tissue sources, which induce cell chemotaxis and collagen synthesis through the Smad pathway and induce osteogenic/odontogenic differentiation through the non-TGFβ-mediated-Smad pathway. Therefore, alkaline treatment has broad applications in coagulation, wound healing [26], and the regeneration of bone, cartilage and dental tissues [11,27].

3.2. Synthesis of an injectable hydrogel capable of loading strong alkaline substances and achieving click-crosslinking

To maintain an alkaline environment of pH 10 at various tissue defects for in situ TGFβ1 activation and tissue regeneration, we engineered an injectable gelatin microsphere hydrogel (MS-Gel) capable of loading strong alkaline substances and achieving click crosslinking (Fig. 2A). The hydrogel was composed of gelatin MSs and a gelatin matrix. MSs with controllable and uniform sizes (50–60 μm) were prepared by polymerization of gelatin droplets generated from a microfluidic flow-focusing device (Fig. S6A). We tested that the type B gelatin possesses 250 nmol/mg amine groups on the backbone. Since glutaraldehyde can strongly crosslink two amine groups, and almost no free amine groups could be detected by the ninhydrin assay, the degree of crosslinking (DCL) was determined to be 125 nmol/mg. A gelatin matrix with a click-crosslinking property was synthesized by incorporating click chemistry pairs of pendant Tr and Nb into polymer backbones using carbodiimide chemistry [23], forming gelatin-Nb (GelNb) and gelatin-Tr (GelTr), respectively. Representative ^{1}H nuclear magnetic resonance (NMR) peaks were assigned to the individual click moieties (Fig. 2B). Fourier transform infrared spectroscopy (FTIR) (Figs. S6B and C) showed that 66 nmol of Tr was attached to each milligram of gelatin polymer, ~2/3 of the amount of Nb (99 nmol/mg). The gelation performance of GelTr and GelNb in 0.01 mol/L pH 7.4 PBS or 0.15 mol/L pH 10 carbonate buffer was investigated using a rheometer. The results showed that under pH 7.4 conditions, gelatin hydrogel was well formed, with an increasing curve of G', while in pH 10 carbonate buffer, gelation was weak or hardly achieved. This finding confirmed that grafted crosslinkers of Tr and Nb lost their reactivity in strong alkaline environments. MSs were then composited with a GelNb-GelTr gelatin matrix solution (Tr:Nb ratio of 1:1) to yield an injectable MS-Gel. The maximal DCL of the gelatin matrix was estimated to be 39.6 nmol/mg, which is ~32% that of MSs. To enable alkaline conditions (pH 10) or neutral conditions (pH 7.4) in MS-Gels, 0.15 mol/L pH 10 Na_2CO_3–$NaHCO_3$ buffer or 0.01 mol/L pH 7.4 PBS possessing normal human osmotic pressure (Table S1) was loaded into the buffer pool of the MSs by diffusion in advance.

MS-Gel was then systematically characterized. Scanning electron microscopy (SEM) was used to examine the characteristic morphologies of 25% MS-Gel (MS:matrix, w/v), 20% MS-Gel and 17% MS-Gel (Fig. 2D–F). Only 20% MS-Gel exhibited an appropriate solid-to-liquid ratio, showing well-interconnected microporous networks with a mean pore size of 40.7 ± 11.4 μm (Fig. 2G). The concentration of gelatin matrix and the alkaline strength in the click crosslinking gelatin matrix dominated the gelation kinetics, which were estimated by rheometry at both pH 10 and pH 7.4 MS-Gel with gelatin matrix concentrations of 4%, 5% and 6%, respectively (Figs. 2H and S6D). The gelation rates were determined by the mean times to a 50% plateau of the storage modulus (Figs. 2I and S6E). Among all samples, the pH 10 MS-Gel with a 5% matrix was cured in 5 min, which was optimal for the expected clinical applications and subsequent in vitro and in vivo experiments. Therefore, 20% MS-Gel composited with a 5% GelTr-GelNb gelatin matrix at either pH 10 or pH 7.4 was used in the following experiments. The compression moduli (pH 10 for 163 kPa and pH 7.4 for 225 kPa) were confirmed to be strong enough to support clinical operations and cell migration (Fig. S6F). The degradability of MS-Gel was then investigated in response to collagenase. As expected, the gelatin matrix alone with a relatively low DCL (32%) degraded rapidly, by ~80% within 24 h. The highly polymerized MSs alone with ~100% DCL exhibited retarded degradation, persisting for as long as 20 days. MS-Gel showed a similar degradation pattern to that of MSs alone. However, it exhibited significantly accelerated degradation on day 1 and day 3, which was attributed to quick loss of the gelatin matrix (Fig. 2J). After gelatin matrix

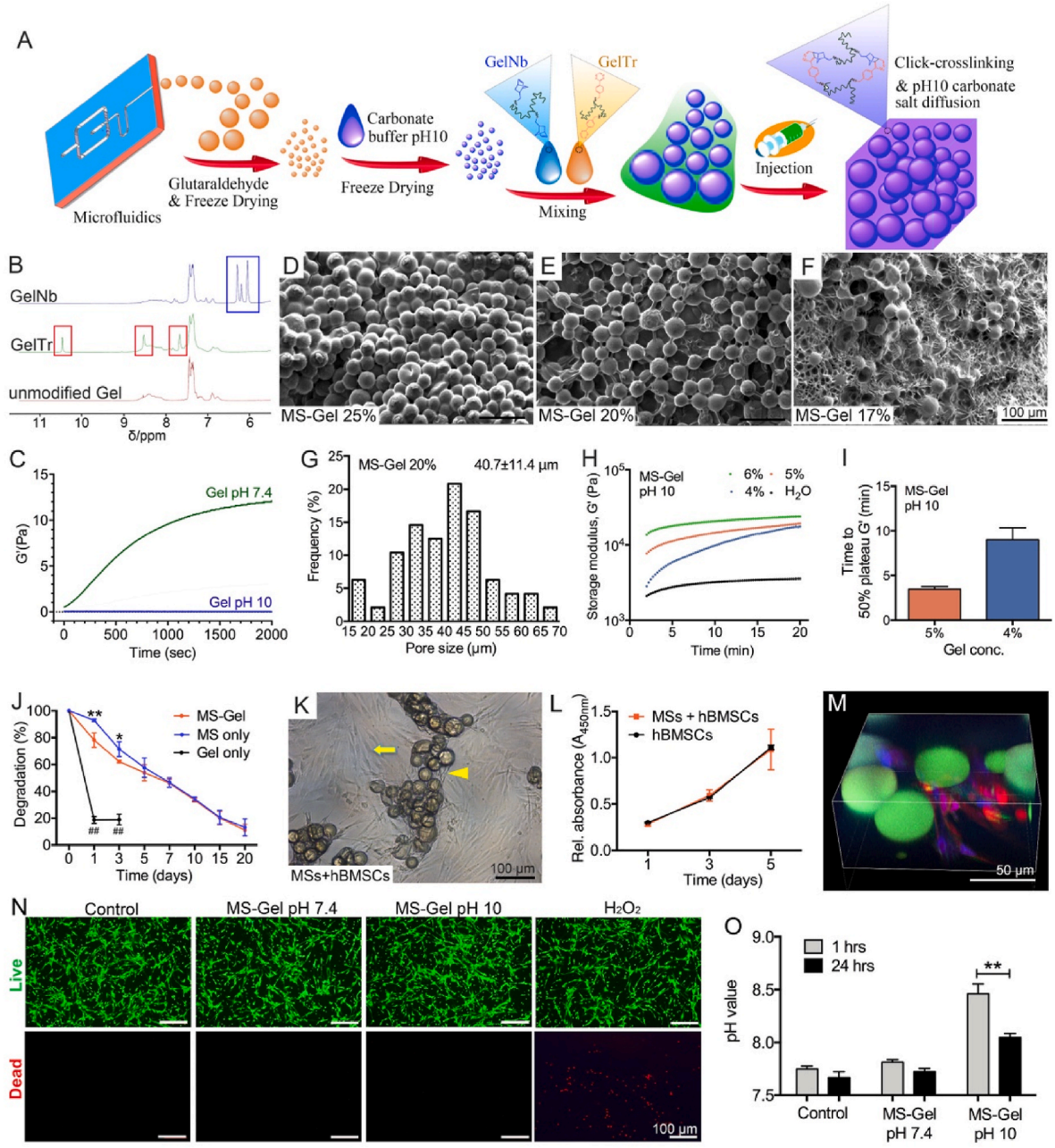

Fig. 2. Synthesis and characterizations of MS-Gel. (**A**) MSs were fabricated by the crosslinking of gelatin microemulsions by microfluidics followed by immersion in Na_2CO_3–$NaHCO_3$ buffer at pH 10 for diffusional loading of carbonate salts. Then, an injectable pH 10 MS-Gel was yielded by mixing the MSs with a GelNb-GelTr gelatin matrix. (**B**) The characteristic peaks of gelatin norbornene (GelNb, blue box) and tetrazine (GelTr, red boxes), along with unmodified gelatin, in ^{1}H NMR spectra. (C) Storage modulus of GelTr-GelNb gelatin matrix in pH 7.4 and pH 10 conditions. (**D** to **F**) SEM images showing the morphology of pH 10 MS-Gel at 25%, 20% and 17% MS:Gel ratios. (**G**) Pore size distribution of 20% pH 10 MS-Gel. (**H**) Storage modulus of pH 10 MS-Gel with gelatin matrix concentrations from 4% to 6%. (**I**): Time to 50% modulus plateau of pH 10 MS-Gel with gelatin matrix concentrations of 4% and 5%. (**J**) Enzymatic degradation curves of MS-Gel, MSs alone and gelatin matrix alone in PBS containing collagenase. (**K**) Digital image of hBMSCs cultured with MSs. (**L**) Growth curve of hBMSCs cultured with MSs. (**M**) Representative confocal microscopy image showing hBMSC adjacency to MS-Gel (red, cytoskeleton; blue, DAPI; green, MSs). (**N**) Fluorescent images showing live (green) and dead (red) cells of hBMSCs cocultured with pH 10 MS-Gel and (**O**) the variation of pH values of the culture media after treatment for 24 h.

degradation, the interspaces should enable stem cell migration and nutrient diffusion. The biocompatibility of MS-Gel was further evaluated by seeding hBMSCs on materials. Cells maintained their characteristic morphology under coculture with MSs (yellow arrow) and grew on the surface of materials (yellow triangle, Fig. 2K). Cell proliferation was not affected by the presence of MSs (Fig. 2L). hBMSCs showed adjacency with increasing elongation on MS-Gels (Fig. 2M). To investigate the influence of nonphysiological pH on hBMSCs viability, we first added 50 μL of pH 10 MS-Gel to the upper chamber of transwell with 200 μL of culture media, and hBMSCs were seeded in the lower chamber (Fig. 2N). The pH value of the culture media (Fig. 2O) quickly increased to 8.46 ± 0.05 in 1 h and slowly decreased to 8.05 ± 0.02 in 24 h. In addition, we directly adjusted the culture medium for hBMSCs to pH 9 or pH 10 using sodium hydroxide (Fig. S5). In both experiments, cell viability was monitored using a live/dead cell assay, and no evident cell death was observed. These results revealed that alkaline MS-Gel possessed a well-organized structure, finely controlled gelation rates, proper enzymatic degradability, strong mechanical properties and excellent

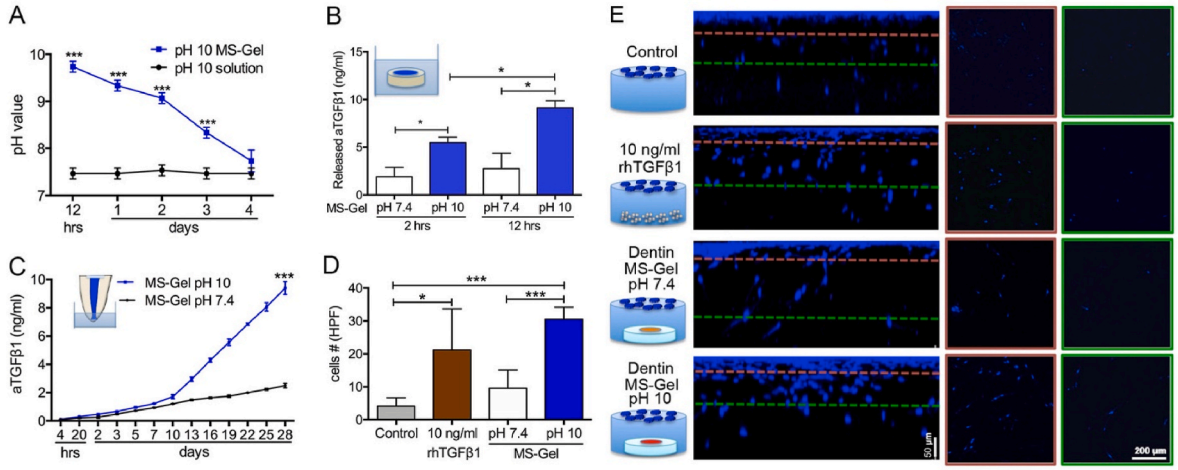

Fig. 3. Effects of MS-Gel on dentin-derived latent TGFβ1 activation for cell migration. (A) pH value changes of pH 10 buffer solution and pH 10 MS-Gel infused into endodontically prepared root canals. (**B**) ELISA was used to measure the release of activated TGFβ1 following pH 7.4 or pH 10 MS-Gel injection in root canals of human tooth root slices. (**C**) ELISA was used to measure the cumulative release of activated TGFβ1 from the apices of pH 7.4 or pH 10 MS-Gel-infused human tooth roots. (**D**) Quantification and (**E**) confocal microscopy images of 3D cell migration assays in 3D collagen gels containing DMEM (control group), 10 ng/mL rhTGFβ1, and dentin slices infused with pH 7.4 MS-Gel or pH 10 MS-Gel. Blue, DAPI.

biocompatibility.

3.3. Alkaline MS-Gel activated dentin-derived TGFβ1 for cell migration

To understand the effects of pH 10 MS-Gel on endogenous latent TGFβ1 activation for complex tissue repair, regenerative models of the pulp-dentin complex in teeth were investigated. We first compared the profiles of pH changes of the pH 10 MS-Gel and an pH 10 alkaline solution injected into endodontically prepared root canals of extracted human tooth roots. The results showed that the pH value of pH 10 MS-Gel decreased to ~9.7 in 12 h, decreased to ~9.3 in 24 h, and decreased slowly to neutrality in 4 days. As expected, the injected pH 10 alkaline solution in root canals was quickly neutralized within 12 h (Fig. 3A). We next evaluated the release of pH 10 MS-Gel-activated TGFβ1 from tooth slices and roots. pH 10 and pH 7.4 MS-Gel was applied for 24 h, followed by immersion in PBS. pH 10 MS-Gel activated 5.6 ± 0.3 ng/mL TGFβ1 in 2 h and 9.4 ± 0.4 ng/mL TGFβ1 in 12 h, which was ~3 times that of the pH 7.4 MS-Gel counterpart (1.8 ± 0.4 ng/mL in 2 h; 2.3 ± 0.8 ng/mL in 12 h) (Fig. 3B). Moreover, accumulated activated TGFβ1 diffused through the root apex in 28 days in response to the pH 10 MS-Gel (9.4 ± 0.3 ng/mL), which was ~4 times more than the amount that diffused in response to the pH 7.4 MS-Gel (2.5 ± 0.1 ng/mL) (Fig. 3C). These results suggested that the alkaline ions in pH 10 MS-Gel were able to diffuse sustainably for effective dentin-derived TGFβ1 activation. Moreover, MS-Gel was able to act as a protein reservoir pool for controllable and prolonged TGFβ1 release.

To confirm the cell chemotaxis of pH 10 MS-Gel-activated TGFβ1, cell migration experiments were conducted in a 3D collagen gel model. MS-Gel-infused tooth slices were embedded at the bottom of a 3D collagen gel, and hBMSCs were seeded on top to observe cell penetration into the 3D collagen gel. Collagen gel containing dentin slices infused with pH 10 MS-Gel induced robust hBMSC migration, and the migrated cell number at 50 μm from the top was comparable to that induced by 10 ng/mL recombinant human TGFβ1 (rhTGFβ1) and much stronger than that in the control group and the pH 7.4 MS-Gel group (Fig. 3D and E). These results indicated that the TGFβ1 released from dentin was activated well by pH 10 MS-Gel. Activated TGFβ1 demonstrated a powerful ability to recruit hBMSCs through the formed concentration gradient.

3.4. Alkaline MS-Gel induced mesenchymal tissue regeneration with proliferating endogenous cells and vasculature in an ectopic rat model

Two distinct in vivo animal models were chosen to demonstrate the potential of pH 10 MS-Gel to achieve tissue regeneration. For the first model, an ectopic regeneration model, endodontically prepared root canals of human tooth roots were rinsed with EDTA and saline, filled with pH 7.4 or pH 10 MS-Gel and implanted in the dorsa of nude rats for 6 weeks. Endodontically prepared empty root canals (without any filling) were used as controls. Hematoxylin and eosin (H&E) staining revealed modest soft tissue formation up to the root canal's middle 1/3 in the control group (Fig. 4A). Abundant newly formed tissue filled the root canals in the representative pH 7.4 or pH 10 MS-Gel samples (Fig. 4B and C). Some remaining MSs were observed in the middle 1/3 of the root canal in pH 7.4 and pH 10 MS-Gel-infused samples (Fig. 4B1, C1), while no MSs were observed in the empty controls (Fig. 4A1). Abundant cells and collagens were present in the representative pH 10 MS-Gel sample (Fig. 4C2) and, to some degree, in the representative pH 7.4 MS-Gel sample (Fig. 4B2), while sparse tissue was observed in the empty control (Fig. 4A2). Remarkably, columnar odontoblast-like cells lined the dentin wall of the representative pH 10 MS-Gel sample (Fig. 4C2). In contrast, sparse flat cells lined the dentin wall in the representative pH 7.4 MS-Gel sample (Fig. 4B2). Trichrome staining revealed loose connective tissue in the empty control (Fig. 4A3, 4). In the representative pH 7.4 MS-Gel sample, the root canal space was filled with sparse collagen and fibroblast-like cells (Fig. 4B3, 4). Remarkably, the endodontically prepared root canal of the representative pH 10 MS-Gel sample showed abundant connective tissue populated by cells and vasculature (Fig. 4C3, 4). Odontoblast-like cells lining the dentin wall in the representative pH 10 MS-Gel sample expressed DSPP and dentin matrix protein 1 (DMP1), hallmarks of odontoblast differentiation (Fig. 4C5-6), while little DSPP and DMP1 expression was observed in the representative pH 7.4 MS-Gel and empty control samples (Fig. 4A5, 6 and 4B5, 6). Relative to the pH 7.4 MS-Gel and empty control, the pH 10 MS-Gel induced abundant cellularity and von Willebrand factor (vWF)-positive blood vessels (Fig. 4A7, 8; 4B7, 8; and 4C7, 8). Quantitatively, the pH 10 MS-Gel group exhibited significantly greater cellularity and significantly more proliferating cell nuclear antigen (PCNA)-positive cells and blood vessels than the pH 7.4 MS-Gel and empty control groups (Fig. 4D–F), suggesting that pH 10-activated TGFβ1 may have augmented mesenchymal tissue regeneration with vasculature and proliferative cells from endogenous cells.

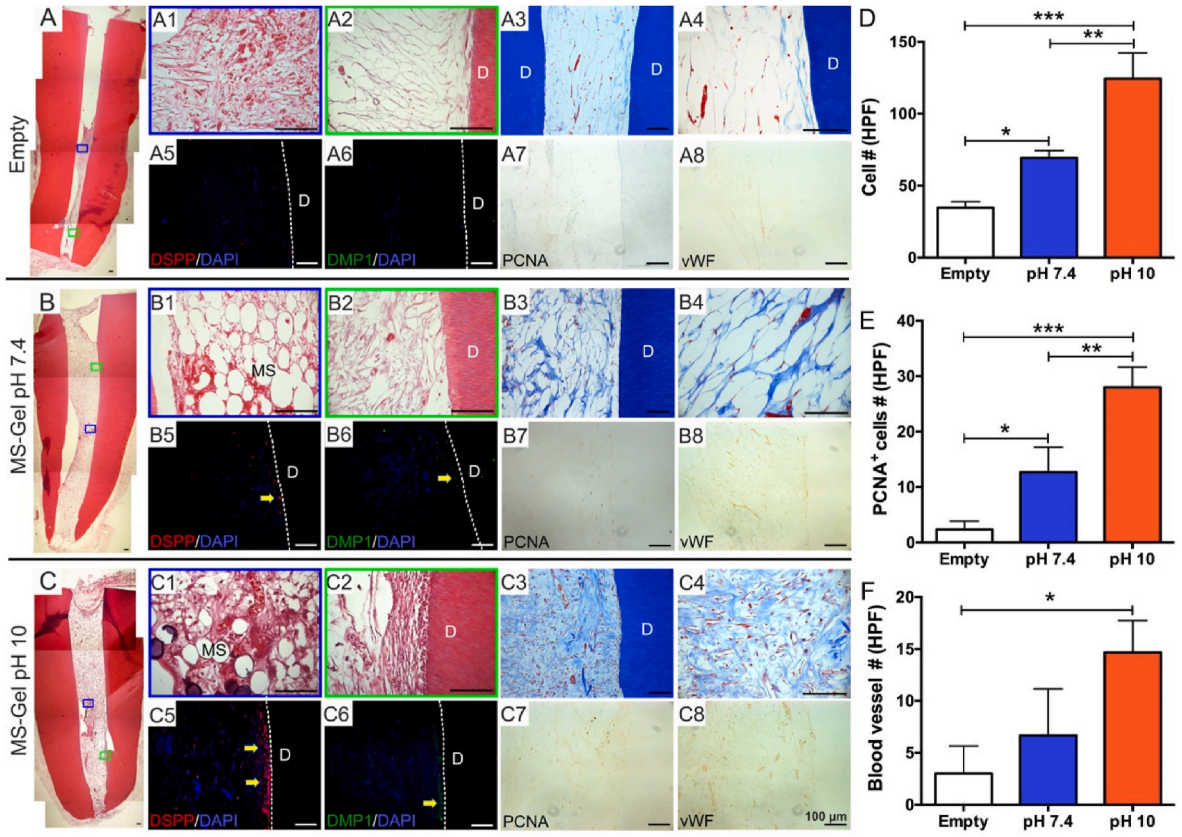

Fig. 4. pH **10 MS-Gel scaffold-activated TGFβ1 induced mesenchymal tissue regeneration with proliferating endogenous cells and vasculature in an ectopic animal (rat) model**. (**A**) Endodontically treated human tooth root sample following 6 weeks of implantation in a rat dorsum without any filling in the root canal (empty). (**A1** and **A2**) H&E staining was performed; the boxed areas are magnified as A1 and A2. (**A3** and **A4**) Masson trichrome staining was performed, and the area is further magnified as A4. (**A5** and **A6**) DSPP and DMP1 immunofluorescence. (**A7** and **A8**) PCNA and vWF immunohistochemistry. (**B**) Endodontically treated human tooth root sample filled with pH 7.4 MS-Gel following 6-week implantation in a rat dorsum. (**B1** and **B2**) H&E staining was performed; the boxed areas are magnified as B1 and B2. (**B3** and **B4**) Masson trichrome staining was performed, and the area is further magnified as B4. (**B5** and **B6**) DSPP and DMP1 immunofluorescence. (**B7** and **B8**) PCNA and vWF immunohistochemistry. (**C**) Endodontically treated human tooth root sample filled with pH 10 MS-Gel following 6 weeks of implantation in a rat dorsum. (**C1** and **C2**) H&E staining was performed; the boxed areas are magnified as C1 and C2. (**C3** and **C4**) Masson trichrome staining was performed, and the area is further magnified as C4. (**C5** and **C6**) DSPP and DMP1 immunofluorescence. (**C7** and **C8**) PCNA and vWF immunohistochemistry. (**D**) Numbers of cells in root canal samples per high-power field (HPF). (**E**) Numbers of proliferating cell nuclear antigen (PCNA)-positive cells in root canal samples. (**F**) Numbers of blood vessels in root canal samples. Scale bar = 100 μm.

3.5. Alkaline MS-Gel induced neurovascular and parenchymal regeneration in a preclinical orthotopic porcine model

To further demonstrate the potential of pH 10 MS-Gel to induce complex tissue regeneration in vivo, we used an orthotopic model to test pulp and dentin regeneration of teeth. Porcine teeth were selected in this study due to their similarities to human teeth in anatomy and physiology. The representative preoperative dental radiographs in Fig. 5A show that the teeth had thin dentin walls and an open apex, indicating tooth roots under development. After dental pulp extirpation, chemomechanical root canal preparation and EDTA and saline conditioning as clinically applied, pH 10 or pH 7.4 MS-Gel was infused into endodontically prepared root canals, and then, coronal restoration was performed. Teeth infused with collagen gel in root canals were used as controls. The postoperative radiograph and μCT images after 3 months showed that the pH 10 MS-Gel-infused tooth acquired thickened root dentin and exhibited apparent root lengthening with apical closure (n = 4 in total 6 samples, Fig. 5B1-D1), which is very similar to natural root development. H&E and Masson trichrome staining (Fig. 5E1-G1) showed that the tooth infused with pH 10 MS-Gel formed vascularized (yellow arrowhead in Fig. 5G1) pulp-like tissues (p) throughout the root canal, and more importantly, a newly generated dentin-like layer (nD) with orderly arranged cells (yellow arrow in Fig. 5G1) was uniformly deposited on the primary dentin wall (D), suggesting de novo pulp and dentin regeneration. No ectopic mineralized tissues were formed within the pulp-like tissues. The cells lining newly formed dentin were positive for DSPP (Fig. 5H1). The regenerated dental pulp contained blood vessel-like structures positive for vWF (Fig. 5I1) and neurite-like sprouts that were double-positive for S100 and protein gene product 9.5 (PGP9.5, Fig. 5J1). The teeth in the control group filled with collagen gel (n = 6 in total 6 samples) and in the pH 7.4 MS-Gel group (n = 6 in total 6 samples) exhibited ectopic intracanal high-density structures (Fig. 5B2-D2, B3-D3). Histological results revealed irregular ectopic mineralization (Em) in the root canal and on the dentin wall (Fig. 5E2-G2, E3-G3). No pulp-like tissue could be distinguished in the root canal. The immunohistochemistry images showed that no dental pulp-like tissue or DSPP-, vWF-, S100- or PGP9.5-positive cells were detected (Fig. 5H2-J2, H3-J3). Our two complementary in vivo models illustrated that transient in vivo alkaline pH perturbation may activate endogenous TGFβ1 for complex tissue regeneration.

4. Discussion

TGFβ1 is secreted and stored in latent forms in multiple species [4,5,28]. The present study began with the discovery that serum TGFβ1 was activated by nonphysiological pH, i.e., pH 2–6 and pH 9–11. The amount

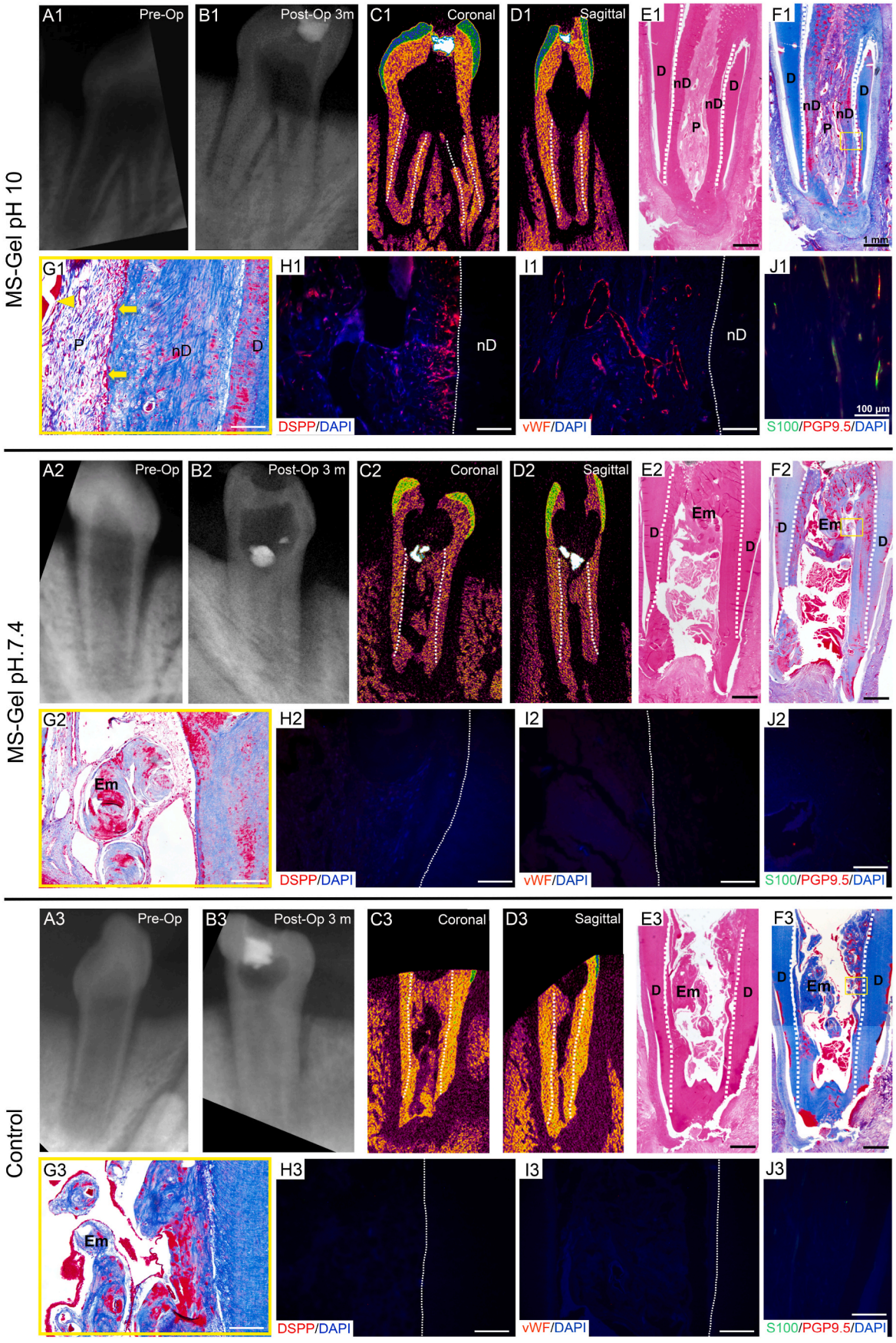

(caption on next page)

Fig. 5. pHn**10 MS-Gel induced neurovascular and parenchymal regeneration in a preclinical orthotopic porcine model**. (**A** and **B**) Radiographic images of representative porcine teeth (A) before treatment and (B) following 3 months of treatment with pH 10 MS-Gel, pH 7.4 MS-Gel and collagen gel as control. (**C** and **D**) μCT images of the pH 10 MS-Gel-treated sample, pH 7.4 MS-Gel-treated sample and collagen-treated sample in the (C) coronal plane and (D) sagittal plane. (**E** to **G**) Histological images of (E) H&E staining and (F) Masson trichrome staining of the pH 10 MS-Gel-treated sample, pH 7.4 MS-Gel-treated sample, and collagen-treated sample. (G) Magnified images of the yellow-coded boxed areas in (F). (**H** to **J**) Immunofluorescence overlay images of (H) DSPP and DAPI; (I) vWF and DAPI; and (J) S100, PGP9.5 and DAPI. (L) vWF and DAPI; and (M) S100, PGP9.5 and DAPI. Abbreviations: D, native dentin; Em, ectopic mineralization; nD, newly formed dentin; P, dental pulp. Scale bars in E, F = 1 mm; in G-J = 100 μm.

of serum TGFβ1 activated ranged from ~19 ng/mL for pH 11–~23 ng/mL for pH 2 over a few hours. Serum TGFβ1 activation has implications for coagulation, wound healing, fibrosis, atherosclerosis and tissue repair, given that blood clots ubiquitously form wound beds [29,30]. Furthermore, the present elucidation of endogenous TGFβ1 activation in bone marrow, cartilage and dentin may lay a foundation for interventional strategies for multiple tissues. Notably, activated TGFβ1 likely forms a gradient that recruits cells, which is a crucial step in tissue repair [31–34]. The modulatory effect of TGFβ1 on stem cell differentiation has been demonstrated in a variety of models. In addition, TGFβ1 plays vital roles in tumor suppression, given its regulation of cancer cell metabolism [7,35].

Although information on TGFβ1 activation has been obtained with multiple biochemical and biophysical methods in vitro, little is known about whether activated endogenous TGFβ1 can be maintained at appropriate levels in tissue defects, and the effects on complex tissue regeneration in vivo remain unclear. Regenerative endodontics, a fascinating and formidable clinical challenge, were used as the experimental model in this study. Over 15 million Americans receive root canal treatment annually to entirely remove pulp tissues due to dental caries and trauma-elicited pulp necrosis. The American Association of Endodontists (AAE) defines regenerative endodontics as “biologically based procedures designed to replace damaged structures, including dentin and root structures, as well as cells of the pulp dentin complex”. To date, approaches for pulp-dentin tissue regeneration have not been well established [36–40]. Although new vital tissue has been found to grow into pulp spaces in some in vivo studies, most of the ingrowing tissues resemble bone, periodontal ligament tissue or cement-like structures rather than pulp-dentin tissues [41–43]. Regenerated pulp-like tissues with blood vessels and nerves are more helpful for restoring pulp immunity, pulp repair and pulp sensitivity. In the pH 10 MS-Gel group, our in vivo data showed that the activation of endogenous TGFβ1 induced the regeneration of organized pulp-like neurovascular stroma that formed orderly mineralized dentin on the canal dentin wall, thereby thickening the root dentin and increasing root length. The pulp-dentin regeneration observed in this study may help to revitalize teeth and enhance the fracture resistance of immature permanent teeth [37]. The European Society of Endodontology (ESE 2016) and AAE (2016) define “increase in root thickness and length” and “positive response to sensitivity testing” as part of the clinical success criteria of regenerative endodontics [44]. Our results lay a foundation for future research on regenerative endodontics. Irregular ectopic intraductal calcification in the control group is considered a pathological or repair process, indicating the lack of a sufficient odontogenic induction signal [38]. It can neither facilitate the function of dental pulp nor provide protection for teeth, let alone real regeneration.

Dentin is known to harbor multiple proteins, including TGFβ1 and TGFβ1-binding proteins [45–47], that can be mobilized and released when injury and diseases occur. Microenvironmental changes may influence the release, exposure and functions of biomolecules, thus offering opportunities for the development of new therapeutic approaches [48]. EDTA is a chelating agent that can remove the smear layer and demineralize dentin. EDTA conditioning may release growth factors from the dentin matrix and promote the adhesion, migration and differentiation of dental pulp cells [49,50]. In this study, pretreatment with EDTA was used to release biomolecules from the dentin matrix, and transient basic pH perturbation may further augment the effect of these released endogenous growth factors on the regeneration of pulp/dentin. Alkaline conditions affected TGFβ1-mediated chemotaxis in the early stage and tissue regeneration in the late stage, while the remaining growth factors were released. In the current study, activated TGFβ1 diffused through the root apex in 28 days in the nanogram range in response to pH 10 MS-Gel. This finding illustrates that after neutralization, the hydrogel can also act as a buffer pool to preserve activated TGFβ1 for continuous release. Not surprisingly, but importantly, alkaline conditions activated endogenous TGFβ1 signals via the Smad pathway, accounting for the observed cell chemotaxis and collagen secretion. In addition, the expression of DSPP, OSX and BSP was upregulated in the alkaline group and was not hindered by Smad signaling inhibitors, suggesting that dentin-derived proteins other than TGFβ1 may also be involved in pulp-dentin regeneration. The process of regenerative endodontics is regulated by a cocktail of substances, including growth factors, chemokines and extracellular matrix molecules [51,52]. The local dissolution of a multitude of bioactive molecules from dentin will play a synergistic effect in repair and regeneration [52]. Among biomolecules, TGFβ1 is often used as a marker substance because it is present in comparably higher amounts than other growth factors [53,54]. It is probable that nonphysiological pH not only activates TGFβ1 but also liberates other tissue-resident cytokines that promote tissue repair [55–58].

After infusing alkaline MS-Gel into root canals, a high pH environment is generated. It can be gradually neutralized by body tissues (such as dentin) and body fluids with certain buffering capacity, which is conducive to subsequent cell migration and growth [59,60]. Some materials, such as bioactive glass and bioceramics, lead to short-term high pH in the local microenvironment in the body and show a good effect of promoting bone repair, which reflects the safety and feasibility of alkaline materials for tissue regeneration [61,62]. Our data on alkaline conditioning-induced pulp-dentin regeneration may also provide some mechanistic basis for bioactive pulp-capping materials that are strongly alkaline in clinical practice, such as MTA (pH ~11.2 at 60 min) and iRoot BP (pH ~11.9 at 60 min) [63,64]. LPL treatment also activates TGFβ1 and promotes mineralization at sites of exposed dental pulp in mice [11]. However, laser-activated TGFβ1 is in the pictogram range and only induces ectopic mineralization at exposed dental pulp [11]. The observed PGP9.5-positive and S100-positive nerve sprouts and vasculature were likely induced by TGFβ1 and other dentin-derived proteins [45,65,66].

In summary, the existence and activation of latent TGFβ1 in multiple tissues (serum, bone marrow, cartilage, tooth) can drive the chemotactic responses of resident stem cells, bypassing the need for exogenous cells or factors. An injectable pH 10 MS-Gel hydrogel was developed, and our tests demonstrated that a mild and prolonged in vivo alkaline pH perturbation can activate endogenous TGFβ1 for the regeneration of complex tissues, such as the pulp-dentin complex. Given the ubiquitous presence and functions of TGFβ1 in human tissues, endogenous TGFβ1 activation may represent a simple interventional approach for tissue repair or disease intervention in multiple tissues. The simplicity of alkaline treatment promises straightforward clinical translation. This work also provides a rational design of biomaterials with non-physiological pH values. Integration of this new method will enable the development of a platform of smart biomaterials with broad applications.

Funding

National Natural Science Foundation of China 81,700953 to S·W.
National Natural Science Foundation of China 81870753 to Y.D.
National Institutes of Health grants R01DE025643, R01DE023112, R01AR065023, R01DE025969 and R01DE026297 to J. J. Mao.

CRediT authorship contribution statement

Sainan Wang: Conceptualization, Methodology, Investigation, Visualization, Funding acquisition, Project administration, Supervision, Writing – original draft, Writing – review & editing. **Yuting Niu:** Conceptualization, Methodology, Investigation, Visualization. **Peipei Jia:** Investigation. **Zheting Liao:** Investigation, Visualization. **Weimin Guo:** Investigation, Visualization. **Rodrigo Cotrim Chaves:** Methodology. **Khanh-Hoa Tran-Ba:** Methodology. **Ling He:** Investigation. **Hanying Bai:** Methodology. **Sam Sia:** Methodology. **Laura J. Kaufman:** Methodology. **Xiaoyan Wang:** Investigation, Visualization. **Yongsheng Zhou:** Supervision. **Yanmei Dong:** Supervision. **Jeremy J. Mao:** Conceptualization, Funding acquisition, Supervision, Writing – review & editing.

Declaration of competing interest

The authors declare that they have no known competing financial interests or personal relationships that could have appeared to influence the work reported in this paper.

Acknowledgments

We thank Q. Guo, P. Ralph-Birkett, and Y. Tse for administrative assistance, and C.H. Lee, S. Tarafder and T. Fiala for their technical assistance with strain-stress measurements and 1H NMR.

Appendix A. Supplementary data

Supplementary data to this article can be found online at https://doi.org/10.1016/j.bioactmat.2021.12.015.

References

[1] J.M. Wells, F.M. Watt, Diverse mechanisms for endogenous regeneration and repair in mammalian organs, Nature 557 (7705) (2018) 322–328.
[2] A.K. Gaharwar, I. Singh, A. Khademhosseini, Engineered biomaterials for in situ tissue regeneration, Nature Reviews Materials (2020) 1–20.
[3] H. Xia, et al., Tissue repair and regeneration with endogenous stem cells, Nature Reviews Materials 3 (7) (2018) 174–193.
[4] J.S. Munger, et al., The integrin alpha v beta 6 binds and activates latent TGF beta 1: a mechanism for regulating pulmonary inflammation and fibrosis, Cell 96 (3) (1999) 319–328.
[5] Y. Zhou, et al., Latent TGF-beta binding protein 3 identifies a second heart field in zebrafish, Nature 474 (7353) (2011) 645–648.
[6] M.A. Travis, D. Sheppard, TGF-beta activation and function in immunity, Annu Rev Immunol 32 (2014) 51–82.
[7] N.F. Brown, J.F. Marshall, Integrin-mediated TGFbeta activation modulates the tumour microenvironment, Cancers (Basel) 11 (9) (2019).
[8] X. Xu, et al., Transforming growth factor-beta in stem cells and tissue homeostasis, Bone Res 6 (2018) 2.
[9] M. Shi, et al., Latent TGF-beta structure and activation, Nature 474 (7351) (2011) 343–349.
[10] J.E. Murphy-Ullrich, M.J. Suto, Thrombospondin-1 regulation of latent TGF-beta activation: a therapeutic target for fibrotic disease, Matrix Biol 68–69 (2018) 28–43.
[11] P.R. Arany, et al., Photoactivation of endogenous latent transforming growth factor-beta1 directs dental stem cell differentiation for regeneration, Sci Transl Med 6 (238) (2014) 238ra69.
[12] X. Dong, et al., Force interacts with macromolecular structure in activation of TGF-beta, Nature 542 (7639) (2017) 55–59.
[13] N. Khalil, TGF-beta: from latent to active, Microbes Infect 1 (15) (1999) 1255–1263.
[14] R.D.A.U. Lins, et al., Biostimulation effects of low-power laser in the repair process, Anais brasileiros de dermatologia 85 (2010) 849–855.
[15] S. Saito, N. Shimizu, F.N.U.S. of Dentistry, Stimulatory effects of low-power laser irradiation on bone regeneration in midpalatal suture during expansion in the rat, American Journal of Orthodontics and Dentofacial Orthopedics 111 (5) (1997) 525–532.
[16] M. Schindl, et al., Induction of complete wound healing in recalcitrant ulcers by low-intensity laser irradiation depends on ulcer cause and size, Photodermatology, photoimmunology & photomedicine 15 (1) (1999) 18–21.
[17] R.M. Lyons, J. Keski-Oja, H.L. Moses, Proteolytic activation of latent transforming growth factor-beta from fibroblast-conditioned medium, Journal of Cell Biology 106 (5) (1988) 1659–1665.
[18] P.D. Brownh, et al., Physicochemical activation of recombinant latent transforming growth factor-beta's 1, 2, and 3, Growth factors 3 (1) (1990) 35–43.
[19] O. Wahlström, et al., Variation of pH in lysed platelet concentrates influence proliferation and alkaline phosphatase activity in human osteoblast-like cells, Platelets 18 (2) (2007) 113–118.
[20] O. Wahlstrom, et al., Acidic preparations of platelet concentrates release bone morphogenetic protein-2, Acta Orthop 79 (3) (2008) 433–437.
[21] H. Mullaguri, et al., Role of pH changes on transforming growth factor-β1 release and on the fibrin architecture of platelet-rich fibrin when layered with biodentine, glass ionomer cement, and intermediate restorative material, Journal of endodontics 42 (5) (2016) 766–770.
[22] L. He, et al., Parenchymal and stromal tissue regeneration of tooth organ by pivotal signals reinstated in decellularized matrix, Nat Mater 18 (6) (2019) 627–637.
[23] S.T. Koshy, et al., Click-crosslinked injectable gelatin hydrogels, Adv Healthc Mater 5 (5) (2016) 541–547.
[24] J. Zhou, J. Rossi, Aptamers as targeted therapeutics: current potential and challenges, Nat Rev Drug Discov 16 (3) (2017) 181–202.
[25] S. Meghji, et al., pH dependence of bone resorption: mouse calvarial osteoclasts are activated by acidosis, American Journal of Physiology-Endocrinology and Metabolism 280 (1) (2001) E112–E119.
[26] S. Liarte, A. Bernabe-Garcia, F.J. Nicolas, Role of tgf- in skin chronic wounds: a keratinocyte perspective, Cells 9 (2) (2020).
[27] M. Wu, G. Chen, Y.P. Li, TGF-beta and BMP signaling in osteoblast, skeletal development, and bone formation, homeostasis and disease, Bone Res 4 (2016) 16009.
[28] S.L. Dallas, et al., Dual role for the latent transforming growth factor-beta binding protein in storage of latent TGF-beta in the extracellular matrix and as a structural matrix protein, J Cell Biol 131 (2) (1995) 539–549.
[29] D.J. Grainger, et al., Release and activation of platelet latent TGF-beta in blood clots during dissolution with plasmin, Nat Med 1 (9) (1995) 932–937.
[30] S. Tsunawaki, et al., Deactivation of macrophages by transforming growth factor-beta, Nature 334 (6179) (1988) 260–262.
[31] C.H. Lee, et al., Regeneration of the articular surface of the rabbit synovial joint by cell homing: a proof of concept study, Lancet 376 (9739) (2010) 440–448.
[32] C.H. Lee, et al., Protein-releasing polymeric scaffolds induce fibrochondrocytic differentiation of endogenous cells for knee meniscus regeneration in sheep, Sci Transl Med 6 (266) (2014) 266ra171.
[33] M.L. Iruela-Arispe, E.H. Sage, Endothelial cells exhibiting angiogenesis in vitro proliferate in response to TGF-β1, Journal of Cellular Biochemistry 52 (4) (1993) 414–430.
[34] P. ten Dijke, H.M. Arthur, Extracellular control of TGFbeta signalling in vascular development and disease, Nat Rev Mol Cell Biol 8 (11) (2007) 857–869.
[35] C. Zhang, et al., Transforming growth factor-β1 regulates the nascent hematopoietic stem cell niche by promoting gluconeogenesis, Leukemia 32 (2) (2018) 479–491.
[36] L. He, et al., Treatment of necrotic teeth by apical revascularization: meta-analysis, Sci Rep 7 (1) (2017) 13941.
[37] X. Wang, et al., Histologic characterization of regenerated tissues in canal space after the revitalization/revascularization procedure of immature dog teeth with apical periodontitis, J Endod 36 (1) (2010) 56–63.
[38] X. Zhu, et al., A miniature swine model for stem cell-based de novo regeneration of dental pulp and dentin-like tissue, Tissue Eng Part C Methods 24 (2) (2018) 108–120.
[39] K. Iohara, et al., Complete pulp regeneration after pulpectomy by transplantation of CD105+ stem cells with stromal cell-derived factor-1, Tissue Eng Part A 17 (15–16) (2011) 1911–1920.
[40] X. Zhu, et al., Immunohistochemical and histochemical analysis of newly formed tissues in root canal space transplanted with dental pulp stem cells plus platelet-rich plasma, J Endod 40 (10) (2014) 1573–1578.
[41] S. Kim, et al., Regenerative endodontics: a comprehensive review, International endodontic journal 51 (12) (2018) 1367–1388.
[42] G. Schmalz, M. Widbiller, K.M. Galler, Clinical perspectives of pulp regeneration, Journal of Endodontics 46 (9) (2020) S161–S174.
[43] X. Wang, et al., Histologic characterization of regenerated tissues in canal space after the revitalization/revascularization procedure of immature dog teeth with apical periodontitis, Journal of endodontics 36 (1) (2010) 56–63.
[44] K. Galler, et al., European Society of Endodontology position statement: revitalization procedures, International endodontic journal 49 (8) (2016) 717–723.
[45] S.Y. Chun, et al., Analysis of the soluble human tooth proteome and its ability to induce dentin/tooth regeneration, Tissue Eng Part A 17 (1–2) (2011) 181–191.
[46] A.J. Sloan, et al., Transforming growth factor-beta isoform expression in mature human healthy and carious molar teeth, Histochem J 32 (4) (2000) 247–252.
[47] L. Graham, et al., The effect of calcium hydroxide on solubilisation of bio-active dentine matrix components, Biomaterials 27 (14) (2006) 2865–2873.

[48] S. Ayoub, et al., The effects of intracanal irrigants and medicaments on dental-derived stem cells fate in regenerative endodontics: an update, Stem cell reviews and reports 16 (4) (2020) 650–660.
[49] K.M. Galler, et al., Influence of root canal disinfectants on growth factor release from dentin, J Endod 41 (3) (2015) 363–368.
[50] K.M. Galler, et al., EDTA conditioning of dentine promotes adhesion, migration and differentiation of dental pulp stem cells, Int Endod J 49 (6) (2016) 581–590.
[51] G. Nikoloudaki, Functions of matricellular proteins in dental tissues and their emerging roles in orofacial tissue development, maintenance, and disease, Int J Mol Sci 22 (12) (2021).
[52] A.J. Smith, et al., Exploiting the bioactive properties of the dentin-pulp complex in regenerative endodontics, J Endod 42 (1) (2016) 47–56.
[53] M. Widbiller, et al., Dentine matrix proteins: isolation and effects on human pulp cells, International endodontic journal 51 (2018) e278–e290.
[54] M. Widbiller, et al., Interactive effects of LPS and dentine matrix proteins on human dental pulp stem cells, International endodontic journal 51 (8) (2018) 877–888.
[55] L. Sadaghiani, et al., Growth factor liberation and DPSC response following dentine conditioning, Journal of Dental Research 95 (11) (2016) 1298–1307.
[56] P. Tomson, et al., Growth factor release from dentine matrix by pulp-capping agents promotes pulp tissue repair-associated events, International endodontic journal 50 (3) (2017) 281–292.
[57] A.A. Atesci, et al., Effect of different dentin conditioning agents on growth factor release, mesenchymal stem cell attachment and morphology, Journal of endodontics 46 (2) (2020) 200–208.
[58] J.A. Khan, et al., Effect of natural and artificial dentin conditioners on the release of vascular endothelial growth factor, Journal of Endodontics 47 (5) (2021) 800–805.
[59] J. Camps, D.H. Pashley, Buffering action of human dentin in vitro, Journal of Adhesive Dentistry 2 (1) (2000).
[60] C.N. Carvalho, et al., Ions release and pH of calcium hydroxide-, chlorhexidine-and bioactive glass-based endodontic medicaments, Brazilian dental journal 27 (2016) 325–331.
[61] L.L. Hench, H.A. Paschall, Direct chemical bond of bioactive glass-ceramic materials to bone and muscle, J Biomed Mater Res 7 (3) (1973) 25–42.
[62] L.L. Hench, I.D. Xynos, J.M. Polak, Bioactive glasses for in situ tissue regeneration, J Biomater Sci Polym Ed 15 (4) (2004) 543–562.
[63] A. Abou ElReash, et al., Antimicrobial activity and pH measurement of calcium silicate cements versus new bioactive resin composite restorative material, BMC oral health 19 (1) (2019) 1–10.
[64] K. Wattanapakkavong, T. Srisuwan, Release of transforming growth factor beta 1 from human tooth dentin after application of either ProRoot MTA or Biodentine as a coronal barrier, Journal of endodontics 45 (6) (2019) 701–705.
[65] S. Yamazaki, et al., Nonmyelinating Schwann cells maintain hematopoietic stem cell hibernation in the bone marrow niche, Cell 147 (5) (2011) 1146–1158.
[66] R.W.D. Gilbert, M.K. Vickaryous, A.M. Viloria-Petit, Signalling by transforming growth factor beta isoforms in wound healing and tissue regeneration, J Dev Biol 4 (2) (2016).